THE PROTEIN SOCIETY

Structural characterization of the catalytic γ and regulatory β subunits of phosphorylase kinase in the context of the hexadecameric enzyme complex

Mary Ashley Rimmer, Owen W. Nadeau, Antonio Artigues, and Gerald M. Carlson*

Department of Biochemistry and Molecular Biology, University of Kansas Medical Center, Kansas City, Kansas 66160

Received 24 July 2017; Accepted 19 October 2017
DOI: 10.1002/pro.3340
Published online 3 November 2017 proteinscience.org

Abstract: In the tightly regulated glycogenolysis cascade, the breakdown of glycogen to glucose-1-phosphate, phosphorylase kinase (PhK) plays a key role in regulating the activity of glycogen phosphorylase. PhK is a 1.3 MDa hexadecamer, with four copies each of four different subunits (α, β, γ and δ), making the study of its structure challenging. Using hydrogen-deuterium exchange, we have analyzed the regulatory β subunit and the catalytic γ subunit in the context of the intact non-activated PhK complex to study the structure of these subunits and identify regions of surface exposure. Our data suggest that within the non-activated complex the γ subunit assumes an activated conformation and are consistent with a previous docking model of the β subunit within the cryoelectron microscopy envelope of PhK.

Keywords: hydrogen-deuterium exchange; mass spectrometry; phosphorylase kinase; calmodulin; oligomeric proteins; molecular modeling

Introduction

Phosphorylase kinase (PhK*) is an $(\alpha\beta\gamma\delta)_4$ hexadecameric enzyme complex of 1.3 MDa that phosphorylates and activates glycogen phosphorylase in the cascade activation of glycogenolysis. The γ subunit (44.7 kDa, 386 amino acids) is the catalytic protein kinase,[1] and

Abbreviations: PhK, phosphorylase kinase; CaM, calmodulin; CaMK, CaM-dependent protein kinase; CBD, CaM-binding domain; CRD, C-terminal regulatory domain; DAPK, death-associated protein kinase; EM, electron microscopy; GHL, glycoside hydrolase-like; HDX, hydrogen-deuterium exchange; HRL, Huntington-elongation-A subunit TOR- repeat like; mAb, monoclonal antibody; MS, mass spectrometer, -try, -tric; PKA, cAMP-dependent protein kinase; and ; TFA, trifluoroacetic acid

Additional Supporting Information may be found in the online version of this article.

Statement: Phosphorylase kinase (PhK) is an $(\alpha\beta\gamma\delta)_4$ hexadecameric complex whose β and γ subunits have previously been shown to be functionally and structurally coupled with each other in the enzyme complex. This article describes the first hydrogen-deuterium exchange studies carried out on these subunits as part of the PhK complex, and compares those results against the known structural and functional features of the β and γ subunits.

Grant sponsor: National Institutes of Health; Grant number: DK32953 to G.M.C; Grant sponsor: KUMC Biomedical Research Training Program to M.A.R.; National Institute of Diabetes and Digestive and Kidney Diseases; Grant number: DK32953; Grant sponsor: University of Kansas Medical Center; Grant number: BRTP.

*Correspondence to: Gerald M. Carlson, Department of Biochemistry and Molecular Biology, MS 3030, University of Kansas Medical Center, 3901 Rainbow Blvd., Kansas City, Kansas 66160. E-mail: gcarlson@kumc.edu

Mary Ashley Rimmer's current address is Center for Biomolecular Science and Engineering, Naval Research Laboratory, Washington, DC 20375

its activity is controlled by the three regulatory subunits: α (138.4 kDa, 1237 amino acids[2]), β (125.2 kDa, 1092 amino acids[2]) and δ (16.7 kDa, 148 amino acids[3]). The major forms of regulation of PhK are its activation by cAMP-dependent protein kinase (PKA), predominantly through phosphorylation of Ser-26 on its β subunit,[4] and its binding of Ca^{2+} to its δ subunit, which is tightly bound, endogenous calmodulin (CaM).[5] Of these two types of activation, that by Ca^{2+} is the most fundamental, in that the phosphorylated enzyme still requires Ca^{2+} for the kinase activity of the γ subunit to be expressed.[6] Although binding of the CaM (δ) subunit within the PhK complex seems to occur largely through interactions with the C-terminal regulatory domain of the catalytic γ subunit (γCRD),[7–9] the binding of Ca^{2+} to δ induces large structural changes throughout the entire PhK complex,[10] and an $\alpha\leftrightarrow\gamma\leftrightarrow\delta$ Ca^{2+}-dependent communication network has been observed within the complex.[11] Also within the PhK complex, the γCRD has been shown to interact with the N-terminal region of the β subunit near its PKA phosphorylation site,[12] and regions of the β and γ subunits that are proximal within the complex have been shown to be structurally coupled to each other and with PhK activation.[13] Moreover, a model has recently been formulated in which non-activated PhK is characterized by an interaction between the γCRD and the nonphosphorylated N-terminus of β, with phosphorylation of the latter weakening that interaction and giving rise to activation of γ.[14]

Subunit interactions within the PhK complex have been characterized through chemical crosslinking[11,15–19] and native mass spectrometry (MS),[20,21] and it has been found that each type of subunit interacts with every other type within the $(\alpha\beta\gamma\delta)_4$ complex.[20] Reconstructions of electron microscopy (EM) images show that the hexadecamer is actually arranged as a dimer of $(\alpha\beta\gamma\delta)_2$ octamers perpendicular to each other, but separated by four bridges, i.e., a pseudotetrahedron.[22,23] Portions of all four subunits have been localized within the complex by EM,[13,23,24] and the four bridges at the core of the complex are known to be composed of β subunits.[21] Less is known, however, about the atomic structures of the individual subunits, particularly within the context of the hexadecameric complex. High resolution structures of CaM (δ) and the catalytic domain of the γ subunit (minus the γCRD) have been solved,[25,26] but in the absence of PhK's other subunits. The α and β subunits are homologous, with two unique regions in α and one in β,[2] and structural models for the individual subunits have been generated.[21,27] These models for both isolated subunits show highly helical, two-domain structures; however, the structure of neither subunit has been examined in the context of the $(\alpha\beta\gamma\delta)_4$ hexadecameric complex. In this current study, hydrogen-deuterium exchange (HDX) is used to evaluate the structure of the β subunit in the context of the entire complex, including ramifications of the β_4 core.

As indicated above, within PhK the β and γ subunits are associated with each other near the N-terminus of β and the C-terminus of γ. The γ subunit is a typical CaM-dependent Ser/Thr protein kinase, with its C-terminus thought to bind the δ subunit (CaM) through one or both of two previously identified high-affinity CaM-binding sites.[7,9] Because the structure of the 87-residue γCRD has not been previously characterized, we have modeled its structure as an extension of the catalytic domain (i.e., full-length γ subunit), and portions of that extension are covered by the HDX of the complete γ subunit as part of the PhK complex.

The structures of the β and γ subunits as members of the $(\alpha\beta\gamma\delta)_4$ PhK complex are evaluated herein by performance of HDX on non-activated PhK. In this technique, the amide backbone hydrogens exchange for deuterium when a protein is incubated in a D_2O buffer. This exchange provides information on the secondary and tertiary structures of specific regions, as well as their surface exposure and dynamics. The multiple subunits of PhK result in 325 kDa of unique sequence, making HDX challenging. Using a sufficiently long gradient to reduce the number of co-eluting peptides, while still keeping the gradient sufficiently short to reduce back-exchange of the deuterons, allowed for significant coverage of the α, β and γ subunits, the first subunit being the subject of the preceding article[27] and the latter two of this article.

Results and Discussion

Of the 325 kDa of unique sequence (a single αβγδ protomer) in the PhK complex, the regulatory β subunit accounts for 125.2 kDa, and the catalytic γ subunit 44.7 kDa. In order to analyze the structures of these subunits in the complex, HDX was performed on intact, non-activated PhK over a time- course from 15 s to 6 h. Although the peptide map of the β subunit yielded 94% coverage and γ 90%, when deuterated peptides with overlapping envelopes or low-intensity peaks were excluded, 72 peptides of sufficient resolution and intensity for analysis remained for β, resulting in a slightly reduced coverage of 76%, and 37 peptides for γ, giving 87% coverage. Despite this, there were enough remaining peptides covering overlapping regions of each subunit for data consolidation, as described in Pascal *et al.*,[28] to narrow the location of exchange to within a few residues (Tables I and II). Following this individual peptide analysis, to facilitate comparison of different regions of the subunits, the extent of incorporation into each peptide was converted to a percent of the total theoretical possible exchange (all residues excluding the first two residues[29] and any prolines are theoretically exchangeable). These percentages

Table I. *Extent Deuterium Incorporation for the β-Subunit*

Data Consolidated Regions[a]	15 s[b] (%D)		10 min[b] (%D)		90 min[b] (%D)		6 h[b] (%D)	
9–33	67.5	High	69.4	High	69.9	High	66.3	High
36–44	65.0	High	74.7	High	–[c]	High	64.1	High
49–52	1.7	Low	7.7	Low	21.7	Low	26.7	Low
53–60	0	Low	0.9	Low	3.8	Low	8.8	Low
61	10	Low	7	Low	30	Low	50	Med
64–87	27.4	Low	42	Med	45.6	Med	43.8	Med
88–99	0	Low	0	Low	0	Low	0	Low
102–125	4.4	Low	4.0	Low	5.8	Low	7.1	Low
128–148	12.6	Low	26.1	Low	38.8	Med	43.6	Med
151–160	4.1	Low	19.2	Low	24.3	Low	28.4	Low
209–220	21.7	Low	40.6	Med	49.2	Med	57.1	Med
223–245	12.5	Low	29.6	Low	33.3	Med	34	Med
248–261	9.4	Low	21.5	Low	24.7	Low	25.7	Low
281–311	10.0	Low	14.9	Low	15.4	Low	17.5	Low
314–332	5.7	Low	11.5	Low	21.5	Low	32.8	Med
333–341	13	Low	51	Med	73	High	72	High
354–371	31	Med	36	Med	42	Med	44	Med
372–373	5	Low	35	Med	35	Med	40	Med
374–392	7	Low	12	Low	17	Low	19	Low
395–408	19.5	Low	29.9	Low	36.1	Med	41.9	Med
409–414	12	Low	25	Low	30	Low	37	Med
415	10	Low	0	Low	20	Low	30	Low
418–439	26.4	Low	45.8	Med	53.1	Med	53.3	Med
442–446	2.6	Low	6.7	Low	18.3	Low	23.8	Low
449–469	10	Low	1	Low	3	Low	6	Low
470–480	52.5	Med	73	High	76	High	75.1	High
483–498	24.4	Low	38.4	Med	45.8	Med	49.4	Med
501–533	4.5	Low	3.6	Low	5.6	Low	3.7	Low
541–575	12.2	Low	23.0	Low	30.1	Low	37.3	Med
596–617	8.8	Low	13.9	Low	14.9	Low	14.7	Low
622–634	–	Low	14.1	Low	11.5	Low	12.4	Low
639–662	14.0	Low	26.7	Low	48.6	Med	41.6	Med
665–669	2.9	Low	0.4	Low	0	Low	0	Low
717–727	26.6	Low	48.1	Med	51.6	Med	50.4	Med
728–732	12	Low	32	Med	42	Med	54	Med
733–736	68	High	68	High	70	High	75	High
745–754	9.2	Low	24.2	Low	46.5	Med	47.3	Med
757–779	17.9	Low	36.6	Med	53.0	Med	56.2	Med
780–786	0	Low	6	Low	10	Low	21	Low
789–802	25.2	Low	56.6	Med	72.5	High	72.5	High
805–819	18.4	Low	36.9	Med	53.8	Med	54.6	Med
822–835	33.7	Med	66.6	High	79.1	High	78.3	High
838–852	16.2	Low	22.2	Low	31.7	Med	34.1	Med
855–866	8.1	Low	25.5	Low	–	Med	46.2	Med
925–933	3.6	Low	11.0	Low	23.0	Low	33.8	Med
936–948	12.5	Low	25.9	Low	33.4	Med	34.3	Med
951–970	16.5	Low	38	Med	45.5	Med	48.1	Med
971–973	43	Med	63	Med	66	Med	73	Med
1012–1043	–	Low	12.3	Low	17.8	Low	22.7	Low
1056–1067	11.8	Low	30.3	Low	–	Med	42.7	Med

[a] Regions showing the deuterated coverage of the entire β-subunit, with the percent deuterium incorporated and the resulting classification of that region listed for each time point. Data consolidation[28] has been applied to all regions, and the number of deuterons incorporated has been converted to percentages. Overlapping peptides used for further resolution are not included. Redundant peptides (same peptide, with different charge) are also excluded; entire time courses for every peptide can be found in the supplementary material.

[b] Four time points, out of the nine, are shown here to represent early, middle and late exchange.

[c] If no data were available for a specific time point, the classification for the peptide that could be reasonably extrapolated from the prior and subsequent time point is listed for that point.

were arbitrarily classified as low (≤ 30%), medium (31–60%), or high (> 60%), which are the descriptors that will be used to discuss the relative exchange in specific regions of the subunits. Tables I and II employ this terminology, with color coding, in presenting the percent exchange into specific regions of the β and γ subunits, respectively, at early, mid, and late times of exchange. The complete time-courses of

Table II. *Extent Deuterium Incorporation for the γ-Subunit*

Data Consolidated Regions[a]	15 s[b] (%D)		10 min[b] (%D)		90 min[b] (%D)		6 h[b] (%D)	
3–25	31	Med	42	Med	41	Med	42	Med
26–30	56	Med	70	High	70	High	70	High
31	70	High	70	High	70	High	70	High
32	30	Low	100	High	90	High	100	High
33–44	4	Low	14	Low	28	Low	37	Med
45–58	24	Low	31	Med	24	Low	24	Low
74–99	19	Low	32	Med	39	Med	45	Med
102–111	19.1	Low	51	Med	53.9	Med	55	Med
114–134	5.4	Low	15.1	Low	29	Low	36	Med
137–141	0	Low	0	Low	0	Low	0	Low
142–156	9	Low	14	Low	22	Low	30	Low
160–170	8.8	Low	30.4	Low	39	Med	47	Med
172–196	23	Low	34	Med	34	Med	36	Med
199–212	19	Low	37	Med	41	Med	42	Med
222–233	15	Low	15	Low	5	Low	8	Low
224–236	25	Low	31	Med	31	Med	28	Low
237	100	High	100	High	100	High	100	High
238	0	Low	20	Low	80	High	100	High
240–267	14	Low	30	Low	41	Med	44	Med
270–279	25	Low	46	Med	49	Med	55	Med
280–289	8	Low	12	Low	20	Low	28	Low
290–295	73	High	79	High	78	High	79	High
296–309	17	Low	26	Low	32	Med	32	Med
317–330	23	Low	55	Med	61	High	61	High
353–369	32	Med	34.6	Med	39	Med	42	Med
381–386	61	High	69.9	High	65	High	62	High

[a] Regions showing the deuterated coverage of the entire γ-subunit, with the percent deuterium incorporated and the resulting classification of that region listed for each time point. Data consolidation[28] has been applied to all regions, and the number of deuterons incorporated has been converted to percentages. Overlapping peptides used for further resolution are not included. Redundant peptides (same peptide, with different charge) are also excluded; entire time courses for every peptide can be found in the supplementary material.
Four time points, out of the nine, are shown here to represent early, middle and late exchange.

exchange into all of the specific peptides used to construct these two data consolidation tables are shown in the *Supplemental Material*.

HDX results for the β subunit

Although a high resolution structure for the β subunit has yet to be experimentally determined, a 3D atomic structure of this subunit has been predicted[21] through a combination of chemical crosslinking, MS, hierarchical modeling using I-TASSER[30–32] and *ab initio* calculations (Fig. 1). In this model, the predominately helical (69%)[21] β subunit structure comprises three separate domains (Fig. 2):[21] an N-terminal phosphorylatable domain (residues 1–40) that is unique to this subunit,[2] a glycosyl hydrolase-like (GHL) domain (residues 41–670),[21,33,34] and a Huntington-elongation-A subunit TOR-repeat like (HRL) domain (residues 671–1092).[21] These three domains together form a toroid-like structure, with the subunit's N- and C-termini proximal to each other.[21] Using as reference information a β_4 complex observed by native MS, known subunit phosphorylation sites, and the approximate location of the subunit in the complex [determined by immunoEM with a β subunit-specific monoclonal antibody (mAb)],[13] the β model was docked successfully into a 3D cryoEM envelope determined for non-activated PhK.[21] As determined by cryoEM, PhK is a large bilobal structure with four interconnecting bridges between the two lobes.[10] Four of the modeled β subunits pack as a dense D2 symmetrical core in the EM envelope, and form numerous contacts with one another, with the GHL domain of each subunit occupying the interior region of one lobe and the HRL domain occupying a single connecting bridge and part of the interior of the second lobe.[21]

For organizational convenience and context, our HDX results will be discussed in relation to this model; however, it must be stated that the HDX results cannot corroborate any model of the β subunit. At best, they can be consistent with it, but presumably with portions of other models as well, especially given the high, experimentally determined helix content of the β subunit.[21] Moreover, it should also be noted that the model is a prediction of the best structure for the β subunit as a free-standing molecule, not as a component of a large, hexadecameric complex. Quaternary interactions within the $(\alpha\beta\gamma\delta)_4$ complex would be expected to affect the structure of β (and γ), and thus the HDX results, in two ways: distortion and protection. The quaternary structure would likely distort the structure of any

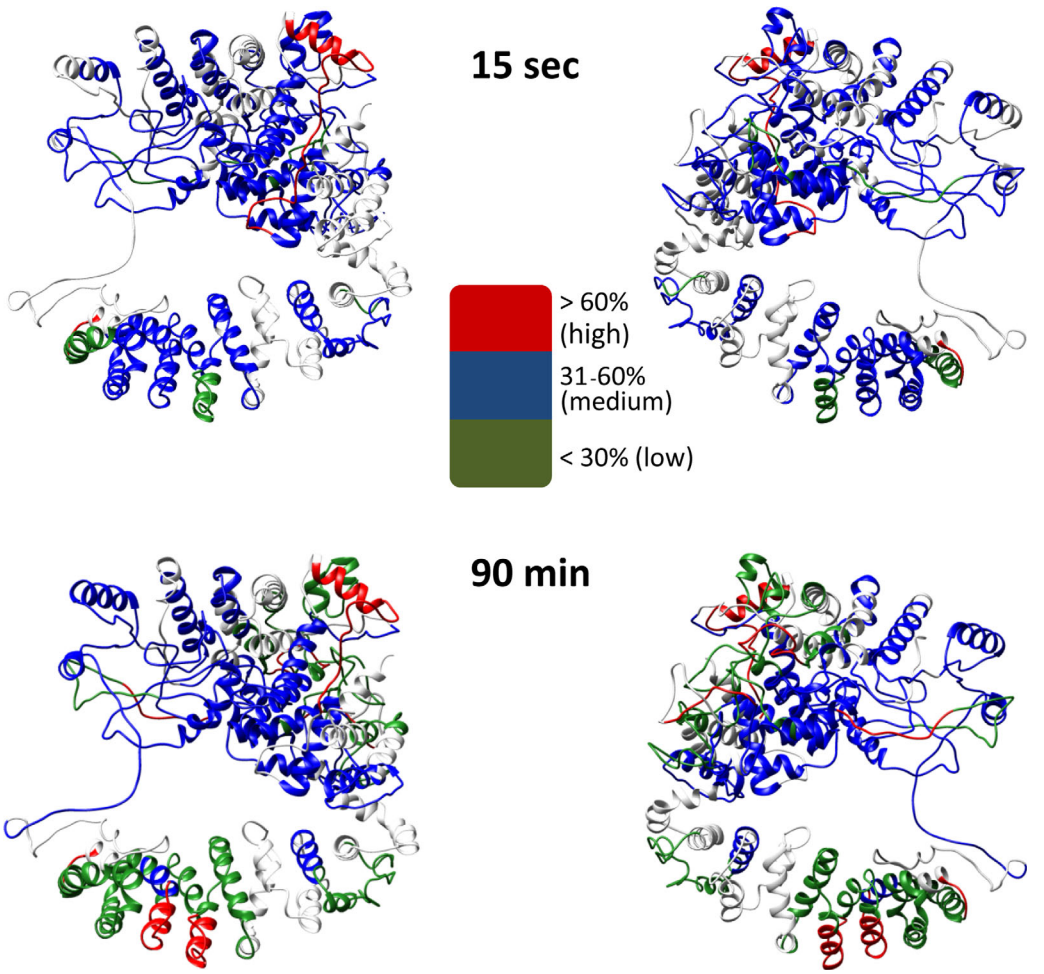

Figure 1. Model of β with HDX results. The exchange results for the non-activated PhK β subunit are mapped onto the theoretical model of β,[21] with low levels of exchange in blue, medium levels in green, and high levels of exchange in red, as indicated by the inset. Upper left, 15-s time point front view, Upper right, 15-s time point back view, Lower left, 90-min time point front view, and Lower right, 90-min time point back view.

free-standing isolated subunit, regardless of whether that structure was generated from modeling, as with β, or from crystallography, in the case of γ. The quaternary structure would also shield from HDX those regions of a subunit directly involved in subunit-subunit interactions. Such protection from exchange is a prominent reason for performing HDX on a complex, as it identifies potential regions of subunit interactions, making it a valuable approach for studying the PhK complex, in which each subunit type interacts with each of the remaining three.[20]

With those caveats described immediately above in mind, the HDX results are largely consistent with the predicted structure of β and its homotetrameric packing in the core of the complex. The vast majority of residues observed in the deuterated peptides underwent low exchange after 15 s, with only 5.7% attaining high levels of exchange during the same time period. Even after 6 h, the percentage of residues undergoing high exchange increased to only 15% (Table I, Fig. 1); and regions of the subunit experiencing higher exchange were consistent with the secondary and tertiary structures predicted and described below for the major domains.

GHL domain. The best matches for the GHL domain in the PDB database were from bacterial and archaeal glucoamylases and glucodextranases, which have a catalytic domain (β residues 41–485) with an $(\alpha/\alpha)_6$ barrel fold and apparent starch-binding domains (β residues 486–670) with mixed secondary structure (Fig. 2).[35] The catalytic domains of these enzymes are α-helical toroids composed of 12 helices with interconnecting loops that alternately pack to form two groups of six helices, with one group arranged externally and the other internally to form a deep active site pocket.[35] Experimental evidence supporting the existence of these domains was revealed in a report demonstrating that PhK tightly binds the GH-15 transition-state inhibitor acarbose, which stimulates PhK's kinase activity and alters cross-linking of its β subunits.[36] With the exception of helix 5 and all but one turn of helix 6, exchange data were available for all of the β

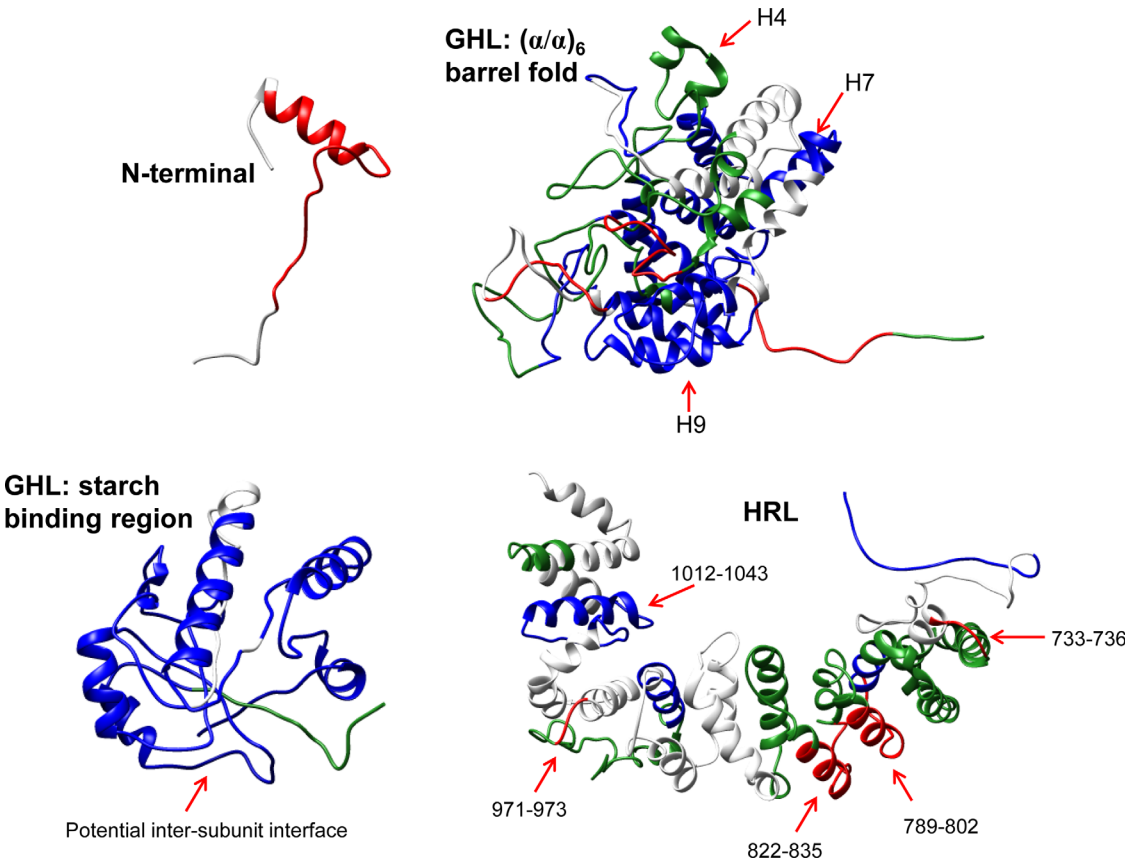

Figure 2. β Subunit model domains and subdomains. The domains of the β model as identified by sequence similarity as discussed in the text are separately shown with HDX results at 90 min. Specific regions of interest discussed in the text are labeled.

subunit $(\alpha/\alpha)_6$ subdomain helices. Levels of deuterium exchange were low for regions of predicted helices 1–3 (residues 45–60, 88–99 and 108–125, respectively), 8 (293–298), 11 (385–391) and 12 (442–454), and all but the first three residues of helix 10 (371–379) (Table I). Predominantly medium levels of exchange were observed for predicted helices 4 (126–137), 7 (235–253), and 9 (310–323), which are denoted by arrows in Figure 2, but these higher levels were only reached at extended times of exchange (≥90 min). Medium exchange was also observed in several regions within predicted loops (64–83, 138–148, 212–234 and 354–370) connecting helices, and high exchange was observed in regions of two loops only (333–341 and 470–480; Fig. 2). Similarly, we recently demonstrated that predicted helices in the GHL catalytic domain of the homologous PhK α subunit exchanged moderately.[27] This pattern was consistent with the simulated unfolding of a related GH-15 family member that unexpectedly underwent thermal denaturation at moderate temperatures,[37] suggesting the α subunit's predicted $(\alpha/\alpha)_6$ barrel to be moderately dynamic. Helices 1, 8, 11 and 7 are thought to be the first to unfold upon thermal denaturation of the GH-15 $(\alpha/\alpha)_6$ barrel;[37] however, exchange for the first three of these predicted helices was very low for the β subunit barrel. Additionally, exchange for helix 7 in the β subunit was predominately low, reaching medium levels only and at later time points, whereas in α its exchange varied from low to high, consistent with its partial melting in the complex.[27] Similar to α, we observed that predicted helices 4 and 9 transitioned from low to medium levels of exchange in the β subunit barrel, despite being packed for the most part internally within each lobe in our model, suggesting β also to be moderately dynamic. These results are consistent with a large body of evidence demonstrating that the β subunit undergoes significant conformational changes in the PhK complex.[10,13,21,38,39] Differences in the HDX for the predicted $(\alpha/\alpha)_6$ barrels for the homologous α and β subunits provide additional evidence supporting differences in the modeled structures generated by us[21,27] and others,[33] with the barrel for α conserving more residues critical for GH catalytic function and that for β containing a small C-terminal insert.[33]

The secondary structure content of the starch-binding subdomain of the GHL differs significantly from the $(\alpha/\alpha)_6$ sub-domain, in that the majority of residues (65%) in the starch- binding subdomain are predicted to compose six large extended loops that

connect six helices ranging from 2–6 turns (Fig. 2). The level of exchange for regions in four of the loops (510–529, 541–575, 611–629 and 665–669) was for the most part low, with medium exchange occurring only after prolonged times for regions of two of the loops (541–575 and 644–653). Given these HDX results, most of the loops are presumably protected from exchange either through subunit interactions or limited exposure to the solvent interface (Fig. 2, arrows), both consistent with the positions predicted for these loops in the lobe interiors of PhK from docking the β models in the PhK cryoEM envelope.[21]

HRL domain. In the atomic model of β docked in the PhK cryoEM envelope, the N-terminus of the HRL domain connects to the GHL domain through an extended loop that passes through a region of low density in the center of PhK to the interior face of the opposing lobe. The loop then transitions to a highly helical structure that occupies roughly half of the interior lobe face and one of the interlobal connecting bridges.[21] With the exception of the regions discussed below, most of this domain underwent low exchange (Fig. 2), progressing to medium exchange at extended times, consistent both with its docking in PhK's quaternary structure and its predicted secondary structure.[21] High levels of exchange were observed for four regions (733–736, 789–802, 822–835 and 971–973) containing predicted loops, with residues 779–811 being previously identified as a loop by partial proteolysis (Fig. 2).[40] The high exchange in these loop regions is consistent with their surface exposure in our docking of β within PhK's quaternary structure.[21]

Site of intrasubunit crosslinking of β. Previously we demonstrated that the N- and C-termini of the β subunit were proximal in PhK by chemically crosslinking Lys-1025 to residues Tyr-51 and Lys-53 with 1,5-difluoro-2,4-dinitrobenzene in the $(\alpha\beta\gamma\delta)_4$ complex.[21] The potential physical interaction between these regions is consistent with the short spacer arm (3–5Å) of this particular crosslinker. HDX within regions containing these residues (49–52 and 1012–1043) revealed extremely low extents of exchange throughout the entire time course, supporting the crosslinking results, and providing additional evidence suggesting the interaction of these two regions of β within the PhK complex.

Exchange in regions of β surrounding sites previously indicated to be exposed: epitope and phosphorylation site. Using truncation mutants to determine the cross-reactivity of a mAb against the β subunit,[13] Nadeau *et al.*[12] narrowed the region in which the epitope occurs to between residues 704–815, and went on to use this information to aid in the docking of the β subunit within the cryoEM envelope.[21] Within this stretch, HDX analysis indicated residues 733–736 (Fig. 2, arrow) to be one of the highest exchanging regions identified in the entire β subunit, even at the shortest times of exchange (Table I). Moreover, these four residues (733–736) are the only ones in this stretch predicted to lack secondary structure, making up a small loop between two helices (Fig. 2). Consequently, this short stretch becomes a strong candidate as the probable epitope.

The key residue targeted by PKA in its activation of PhK and glycogenolysis is Ser-26 of the β subunit,[4] which lies within the N-terminal regulatory domain of β, residues 1–31.[2] This domain appears to mediate an important interaction with the γCRD that keeps the activity of γ from being expressed in non-activated PhK; upon phosphorylation, the inhibitory function of this region is released, resulting in activation of the PhK complex.[14] Due to the requirement for the β regulatory domain to be exposed and accessible to PKA to allow the phosphorylation of Ser-26, it was expected that this region should undergo a high level of exchange. Indeed, the stretch from 9–33 and the adjacent 36–44 are among the highest exchanging regions in the β subunit at short times (Fig. 2). Besides being the regulatory domain, the first 31 residues of β are unique from its largely homologous α subunit, and were initially hypothesized as being surface exposed based on a relatively large percentage of hydrophilic residues.[2] Later, partial proteolysis suggested that this region was on the surface of PhK,[40] which is confirmed by these high levels of exchange.

HDX results for the γ subunit

The catalytic γ subunit of PhK is a Ser/Thr CaM-dependent protein kinase (CaMK). The CaMK family comprises over 70 members,[41,42] making it one of the largest families in the vertebrate kinome. CaMK's have autoregulatory domains (CRD's) that are located C-terminal to their catalytic domains and range between 40 and 50 residues in length.[43,44] In most members, the CRD interacts with the catalytic domain in the absence of Ca^{2+}, either blocking or distorting the kinase active site. This inhibitory interaction is generally relieved by phosphorylation of, and/or CaM-binding to, the CRD.[43] The γ subunit has three domains: its N-terminus, a catalytic domain, and its CRD. Its N-terminus (20 residues) is unique to this kinase.[1] Moreover, based on its large size (96 residues) and multiple subunit interaction sites,[12] the CRD of γ is also unique when compared to other CaMK's.[43] In contrast, the catalytic domain (residues 21–289) shares ∼ 38% homology with the catalytic domains of other CaMK's, including CaMKIIδ[44] and death-associated protein kinase (DAPK). High resolution structural information is available only for the catalytic domain; thus, HDX results will be discussed in reference to both the

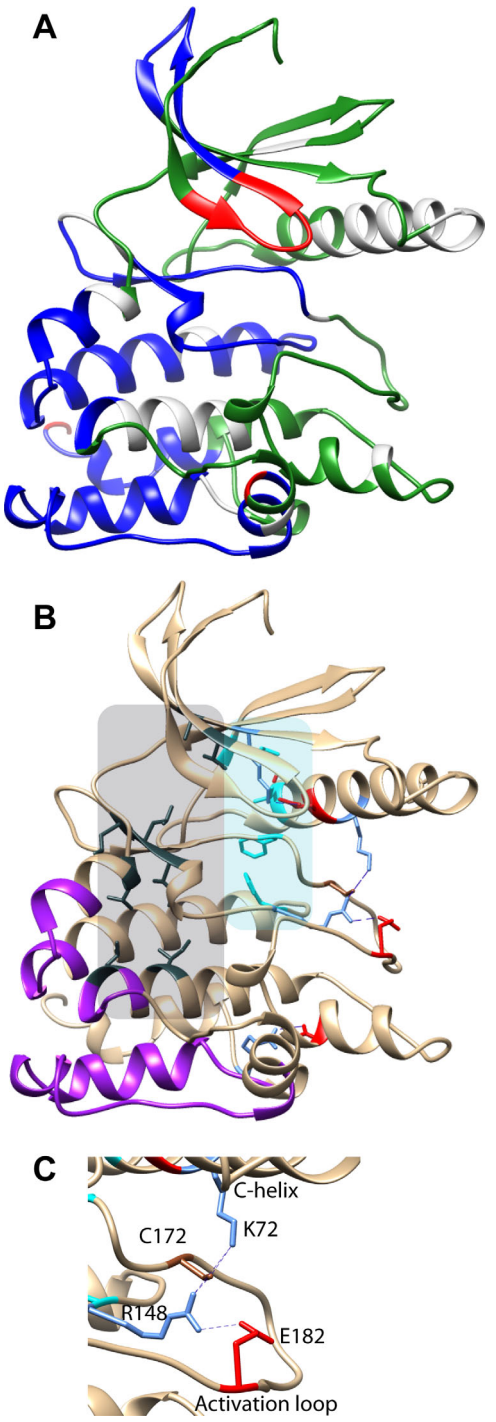

Figure 3. HDX analysis of the γ subunit catalytic domain. (A) Crystal structure (PDB entry 1PHK) of the catalytic domain of PHK γ,[26] with HDX results at 10 min mapped onto the structure (colors as in Fig 1). (B) Structural features of the catalytic domain, including hydrophobic residues composing the R (cyan) and C (slate gray) spines, with the side chains colored (as in Fig. 1). The region of this domain implicated as a subunit contact region[40] is indicated by the purple ribbon structure. (C) Magnified view of the stabilizing interaction network between the C-helix and activation loop of the catalytic cleft.

crystal structure of the catalytic domain (Fig. 3) and a model of the full-length subunit (Fig. 4) constructed by a multiple threading approach using I-TASSER.[32]

N-terminal insert: 1–20. In two different crystal structures of the isolated catalytic domain of γ containing the intact N-terminal insert (with respect to PKA[26,45]) of 20 amino acids, the first 13–14 residues of the N-terminus lack sufficient density for structural determination.[26] On the basis of the position and orientation of the remaining residues in the N-terminus, showing them to project into the solvent, it was hypothesized that these terminal residues were mobile.[26] Our HDX analysis of this region of γ in the context of the entire PhK complex is consistent with this hypothesis, showing a region (residues 3–25) that includes the N-terminus to undergo medium exchange (31–42%) throughout the entire time course [Fig. 3(A)]. These results suggest this region to be relatively solvent accessible and unlikely to be a subunit interaction site in the non-activated conformer of PhK.

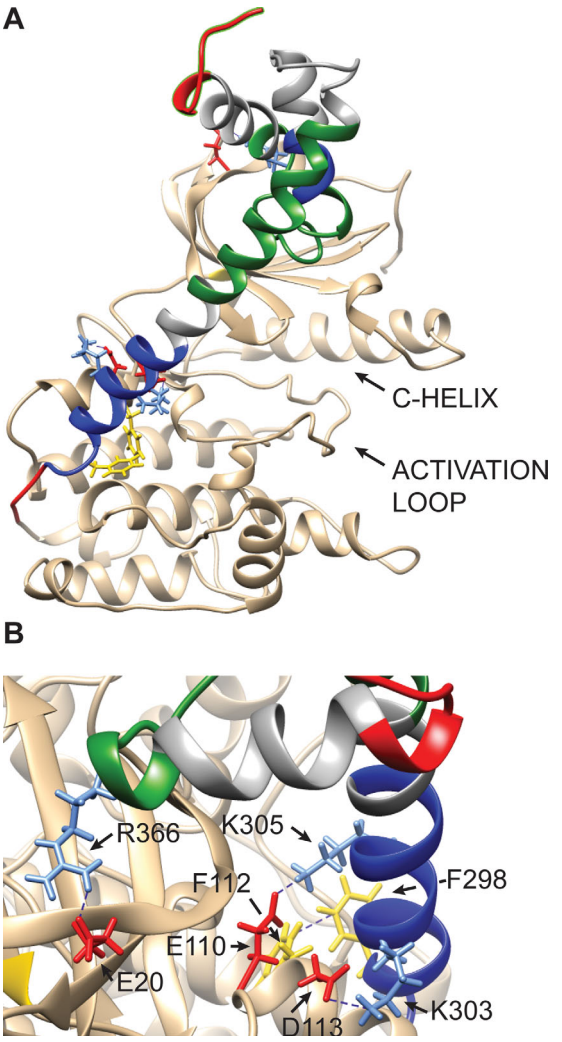

Figure 4. I-TASSER threading model of the full-length γ subunit. (A) Catalytic domain (tan) with CRD (grey) overlaid with the exchange results at 10 min (colors as in Fig 1). (B) Expanded view of side chain contacts between residues from the catalytic domain and the γCRD.

Catalytic domain: 21–298. A comparison of the crystal structures of the catalytic domains of PKA and PhK γ, which have 36% sequence identity,[1] show γ to have the typical bilobal protein kinase fold, namely an N-terminal lobe with mixed α-helical, β-sheet secondary structure, connected through a flexible hinge to a large primarily helical C-terminal lobe. A large catalytic cleft is at the interface between the lobes, with nucleotide and protein substrate binding occurring primarily at sites in the N- and C-terminal lobes, respectively.[45] Active site accessibility is determined by the positions of the lobes with respect to each other, and a translation of approximately 9Å, progressing from an open to a closed conformation, occurs when ATP is bound in the active site cleft.[46] The catalytic domains of protein kinases are dynamic structures, in which conformational transitions are controlled by a flexible grouping of hydrophobic residues, termed spines,[47–49] that form a 3D network of interactions[46] that traverse the kinase core from the F-helix in the C-lobe to the extended β sheet of the N-lobe [Fig. 3(B)]. Two distinct groupings of hydrophobic residues have been characterized, the regulatory (R) and the catalytic (C) spines,[46] both of which are conserved in eukaryotic protein kinases.[46–49] Full assembly of the R spine is a characteristic of activated kinase structures, and is observed in crystal structures of the isolated catalytic domain of γ, which is constitutively active as a free truncated subunit.[8] Disruption of this spine leads to kinase inactivation.[46]

The R spine of the γ subunit of PhK comprises four residues: His-147, Phe-168, Leu-77 and Leu-89. HDX in the regions containing His-147 and Phe-168 was low through 10 min, with the former region remaining at this level for 6 h, and the latter slowly increasing to medium exchange (Table II). The region containing Leu-77 and Leu-89 (residues 74–99; Table II) comprises approximately 1.5 turns of a helix (74–80), a connecting loop (81–88) and part of a β-sheet (89–99), with both residues occupying positions near the loop junctions . A shell surrounding the R spine is important for kinase regulation, and in PKA includes residues Met-118 and Met-120, while other protein kinases also contain a conserved Met diad.[50] In some of these kinases, mutation of the second Met to Phe has been shown to lead to activation,[51] and in the γ subunit of PhK the second Met equivalent is, in fact, Phe-103.[1] The low to moderate exchange observed for these regions in γ suggests the presence of a fully or nearly intact spine, indicative of an activated conformation, and/or low solvent exposure.

The C-spine, which comprises residues Ala-26, Val-33, Leu-156, Leu-157, Leu-111, Ile-155, Leu-222 and Ile-218 in γ, is assembled in the presence of adenine analogs, and couples β2 and β3 in the N-lobe with helices D and E in the C-lobe through contacts with the adenine and ribose rings.[46] HDX coverage was measured for all but two of these residues, with low to medium levels of exchange observed for the majority of residues detected. Despite the absence of ATP, the exchange levels for these residues are again consistent with low solvent exposure and/or an assembled spine.[46]

The activation loop for the active site of γ, residues 178–185, is part of a long extended loop (167–193)[26] that begins and ends with two highly conserved motifs, DFG and APE, respectively.[1] Glu-193 in the APE motif forms a salt bridge with Arg-275, which lies in a second loop between the H and I helices.[26] In PKA disruption of this interaction by mutation leads to a significant decrease in its activity.[52] We observed that regions containing these loops were initially low exchanging, transitioning to medium exchange at later time points, consistent with the presence of the stabilizing salt bridge.

Typically, the activation loops of kinases in the active state are phosphorylated, resulting in the formation of an ion pair between the phosphorylated residue and a positively charged residue at the N-terminus of Helix C (e.g., phospho-Thr-197 and His-87 in PKA). In γ, however, the key phosphorylatable residue is replaced by Glu-182, providing another indication that its basal state is activated.[26] Unlike phospho-Thr-187 in PKA, Glu-182 in γ does not form any direct contacts with the C-helix, rather it is indirectly linked to this helix through a previously described network of interactions[26] that includes residues Arg-148 and Cys-172 in loops proximal to the active site and Lys-72 in Helix C [Fig. 3(C)]. Glu-182 forms an ion pair with Arg-148, which is proximal to Cys-172 (3.47Å), and Cys-172 is within H-bonding distance (2.73Å) with Lys-72 in the C-helix [Fig. 3(C)], mimicking the stabilizing interaction between the activation loop and helix C in PKA.[26] Despite Arg-148, Cys-172 and Glu-182 being in loops, we observed that the regions containing them exchange at low levels initially, followed by medium exchange throughout the time course. Further, although exchange for Lys-72 could not be measured, regions bracketing it underwent low or low to medium exchange. The sum of our exchange data for these four residues is consistent with the proposed stabilizing interaction network described above and with the constitutive activity observed for the isolated γ subunit in solution,[8] Moreover, these results are also consistent with previous findings,[53,54] demonstrating that reduced HDX rates for residues peripheral to the active site are markers for kinase activation.[53,54]

The C-helix is a structural integrator whose spatial position influences the dynamics and activity of protein kinases.[55] It contains one of the spine

residues, which in γ is Leu-77, and any movement of the helix that displaces this residue from the spine leads to inactivation.[56] Similar to the interaction in PKA, helix C in γ is stabilized by a conserved salt bridge (3.6 Å) between Lys-48 and Glu-76 and the loop connecting this helix to β4. Regions containing these two residues predominately undergo low to medium exchange, consistent with the presence of this stabilizing interaction in γ; however, many of the contacts between helix C and the remainder of the core that are observed in PKA are missing in γ. As discussed above, stabilization of the C-helix through interactions with the activation loop appears to occur through contacts that are unique to γ. Taken together, our results indicate for the first time that the γ subunit is catalytically competent in the non-activated $(\alpha\beta\gamma\delta)_4$ complex, i.e., activation results from deinhibition caused by the release of quaternary constraints.

There are three inserts in the catalytic domain of γ that do not correspond to the sequence of the homologous PKA, namely residues 60–66, 196–201, and 252–255. The last two inserts were observed in the HDX data. In the γ crystal structure, insert 196–201 comprises one turn of a helix and connecting loop, which project directly into the solvent just below the activation loop.[26] Several residues (196, 199–201) of this region and residues directly flanking it undergo low levels of exchange at 15 s, increasing to medium levels at 5 min and for the remainder of the time course. The region encompassing residues 252–255 shows similar levels of exchange, remaining at low extent until 90 min and increasing only to medium after that. This region includes one-half turn of a helix and part of a connecting extended loop that also project out into the solvent in the γ crystal structure.[26] The level of exchange for both of these inserts and their solvent-exposed positions in the crystal structure suggest the possibility that they may be near subunit interaction sites in the $(\alpha\beta\gamma\delta)_4$ complex.

Using EM in conjunction with a mAb against the γ subunit, the epitope, identified as being somewhere within the stretch from 277–290, was shown to be located centrally on the interior lobes of the PhK complex.[13] To be accessible to the antibody, this region must be surface exposed, and we find that residues 270–279 rapidly undergo medium levels of exchange. In contrast, residues 280–289, immediately adjacent to this region, remain low exchanging throughout the entire time course, suggesting the actual epitope is located N-terminally in the 277–290 stretch.

From mapping partial proteolysis loops, carboxymethylation footprinting, the mAb binding site, and known sites of substrate interaction onto the crystal structure of the γ subunit, we identified a region on γ that showed no overlap with any of these experimentally identified surface exposed regions. This region was hypothesized to be a site of interaction of the γ subunit with the remainder of the PhK complex.[40] In the tertiary structure of γ, this proposed anchoring region comprised three stretches of residues in the C-terminal lobe, on the opposite side of the active site near the "bottom" of the subunit: 1) a loop connecting the D and E helices, 2) the C-terminus of helix F and a portion of the loop connecting it with helix G, and 3) helix H and the two loops that bracket it [Fig. 3(B)]. In our HDX data, all three of these regions undergo low levels of exchange at 15 s, and the majority of the residues remain at low levels of exchange throughout the time course [Fig. 3(A)]. A few of the residues reach medium levels of exchange, but even those do not get above low levels until at least 10 min or later in the time-course. These data are consistent with the hypothesis that these three regions of γ do, in fact, represent an area in which it interacts with other subunits within the complex.

The C-terminal regulatory domain (γCRD): 299–386. The γCRD has no sequence homology with other protein kinases, and there is no high resolution structural information for this domain. It has, however, been shown to interact with all three of the regulatory subunits in PhK.[12] To gain further insights into the binding interactions of the γCRD with other subunits, we constructed an atomic model [Fig. 4(A)] of the full length γ subunit using the I-TASSER multiple threading approach.[31] The top 10 templates in the PDB database that corresponded to the final predicted structure for γ included two other CaMK's complexed with Ca^{2+}/CaM: DAPK and CaMKIIδ. The modeled structure of the γCRD and its position with respect to the catalytic domain most closely matched the CRD of DAPK in complex with Ca^{2+}/CaM,[43] although a number of stabilizing contacts between the CRD and the catalytic domain observed for CaMKIIδ were also conserved in the γ model. For example, disruption of hydrophobic interactions between Phe-98 and Phe-292 in CaMKIIδ by mutating either residue leads to activation of the kinase,[44] and similar interactions between the corresponding residues in the homologous γ subunit [Phe-112 and Phe-298; Fig. 4(B)] are suggested by their proximity (3.6 Å). CaMKII residues Glu-96 (PhK γ Asp-113) and Arg-297 (γ Lys-303) form a salt bridge, which is mirrored by a predicted ion pair [Fig. 4(B)] between these corresponding residues in γ at a distance of 2.7 Å. Two additional non-conserved stabilizing contacts between the γCRD and catalytic domain are predicted [Fig. 4(B)] between Lys-305 and Glu-110 (2.8 Å), as well as between Arg-366 and Glu-20 (1.83 Å). HDX is low, especially at early time points, for most of the peptides containing the eight residues indicated above (Table II), which is consistent with their proposed intra-subunit interactions.

Although both Arg-366 and Glu-20 are located on peptides that undergo medium exchange, they are bracketed by high-exchanging peptides, consistent with their supplying a stabilizing salt-bridge. Such a salt bridge would connect the N-lobe of the catalytic domain of γ with its CRD, mimicking the known stabilizing salt-bridge observed between the same domains in the crystal structure of DAPK complexed with Ca^{2+}/CaM.[43]

A large body of work has demonstrated a direct linkage between the γCRD and the δ subunit. The region of the γ subunit that interacts with the δ subunit was initially localized to its C-terminal one-quarter (residues 290–386) by truncation,[8,57] synthetic peptides[7] and crosslinking.[9] The truncated γ subunit missing the γCRD is active, but insensitive to Ca^{2+}/CaM.[8,57] Screening of the C-terminal quarter of γ for potential high affinity CaM-binding sequences through the use of overlapping synthetic peptides revealed two distinct, non-overlapping CaM-binding domains (CBD's).[7] The more N-terminal CBD (N-CBD) stretches from residues 297–331 and the more C-terminal CBD (C-CBD) from 337–366. Although it is not known whether only one, or both, of these CBD's interact with the δ subunit within the PhK complex, we previously gained direct evidence of an Asp-Lys salt-bridge between δ and the N-CBD of γ through the zero-length crosslinking of δ Asp-93 and γ Lys-325 within the complex.[9] The exchange coverage we observed for the two CBD's (Table II) was 77% for the N-CBD (both termini covered similarly, but with a 7-residue gap in middle) and 47% for the C-CBD (the C-terminal half). The least exchange observed within the CBD's was for the N-terminal portion of the N-CBD, with peptide 296–309 showing low exchange for up to 30 min (28% exchange) and only 32% exchange after 6 h (Supporting Information, Fig. S2). Thus, as with zero-length crosslinking, our exchange results support the binding of δ to the N-CBD of γ within the PhK complex. We cannot, however, rule out the participation of the C-CBD in the binding of δ, inasmuch as we did not observe peptides from within the N-terminal half of the C-CBD. Moreover, it should be noted that the binding of δ within the PhK complex is likely to be dynamic, in that single molecule trajectory analyses of PhK containing δ subunit labeled at its N- and C-termini with a fluorescent donor-acceptor pair showed that subunit to repeatedly jump back-and-forth between extended and compact conformational substates under constant conditions.[58] The repeated alternate binding of δ to first a single CBD and then to two could produce such a result. Multiple non-contiguous interactions between CaM and several of its protein targets have been characterized,[59,60] e.g., small conductance Ca^{2+}-activated potassium channels.[59] Unlike most CaM targets, both the potassium channel and PhK bind CaM in the absence of Ca^{2+}, but are activated only in its presence.[5,61] This form of CaM binding is atypical with respect to other CaMK members, which bind (and are activated by) CaM only in the presence of Ca^{2+}.[41,43] Moreover, unlike any other CaMK's, the γ subunit of PhK functions as part of a large complex with three additional regulatory subunits, including the β subunit, which is predominate in the activation of PhK through phosphorylation.[4,62]

As discussed above, the structural and functional coupling of the β and γ subunits in the $(\alpha\beta\gamma\delta)_4$ complex has been characterized by multiple methods.[12–14] Although crystal structures of the isolated catalytic domain show it to contain all the structural elements of an activated kinase,[26] the HDX results herein also suggest a catalytically competent conformation of γ in the non-activated PhK complex. The activation (deinhibition) of the γ subunit[16] through the binding of Ca^{2+} by δ and the phosphorylation of β at its N-terminal region[13] occurs concomitantly with a parallel tier of conformational changes that increase the solvent accessibility of portions of γ.[16] Such an increase in accessibility is corroborated by the preferential binding of γ, as well as β, by subunit-specific mAb's in phospho-activated conformers of PhK[13] and by the increased chemical modification of γ in PhK complexed with Ca^{2+}.[16] Although the structural details of the coupling between β and γ that is associated with PhK's activation remain largely unknown, we previously demonstrated through chemical crosslinking that Arg-18 of β, which is in its N-terminal phosphorylatable region, and K-303, in the N-CBD of γ, are proximal in the PhK complex.[12] In that same report, we showed that the crosslinking of these two residues within the complex was inhibited by a peptide corresponding to the N-terminal 22 residues of β. Moreover, this same peptide not only crosslinked with γ K-303 in the complex (i.e., the same residue targeted by its parent β subunit in the PhK complex), it was also phosphorylated by PhK (Ser-11 is an autophosphorylation site),[2,12] consistent with the active site and N-CBD of γ and the phosphorylatable region of β all being proximal. The sum of these results suggests a communication network involving the phosphorylatable N-terminus of β, the γ N-CBD, and δ; and in fact, the phosphorylation of PhK reduces its stringency for activation by Ca^{2+},[63] presumably mediated by the N-CBD.

Materials and Methods

All materials and methods pertaining to performing HDX on the non-activated PhK were as described in the preceding article.[27]

Modeling/threading for full-length γ subunit

Threading models of the γ subunit were generated using the I-TASSER unified platform for automated protein structure and function prediction.[27–29]

References

1. Reimann EM, Titani K, Ericsson LH, Wade RD, Fischer EH, Walsh KA (1984) Homology of the gamma subunit of phosphorylase b kinase with cAMP-dependent protein kinase. Biochemistry 23:4185–4192.
2. Kilimann MW, Zander NF, Kuhn CC, Crabb JW, Meyer HE, Heilmeyer LM Jr (1988) The α and β subunits of phosphorylase kinase are homologous: cDNA cloning and primary structure of the beta subunit. Proc Natl Acad Sci USA 85:9381–9385.
3. Grand RJ, Shenolikar S, Cohen P (1981) The amino acid sequence of the delta subunit (calmodulin) of rabbit skeletal muscle phosphorylase kinase. Eur J Biochem 113:359–367.
4. Yeaman SJ, Cohen P (1975) The hormonal control of activity of skeletal muscle phosphorylase kinase. Phosphorylation of the enzyme at two sites in vivo in response to adrenalin. Eur J Biochem 51:93–104.
5. Cohen P, Burchell A, Foulkes JG, Cohen PT, Vanaman TC, Nairn C (1978) Identification of the Ca^{2+}-dependent modulator protein as the fourth subunit of rabbit skeletal muscle phosphorylase kinase. FEBS Lett 92: 287–293.
6. Ozawa E (1973) Activation of phosphorylase kinase from brain by small amounts of calcium ion. J Neurochem 20:1487–1488.
7. Dasgupta M, Honeycutt T, Blumenthal DK (1989) The γ-subunit of skeletal muscle phosphorylase kinase contains two noncontiguous domains that act in concert to bind calmodulin. J Biol Chem 264:17156–17163.
8. Harris WR, Malencik DA, Johnson CM, Carr SA, Roberts GD, Byles CA, Anderson SR, Heilmeyer LM, Jr, Fischer EH, Crabb JW (1990) Purification and characterization of catalytic fragments of phosphorylase kinase γ subunit missing a calmodulin-binding domain. J Biol Chem 265:11740–11745.
9. Jeyasingham MD, Artigues A, Nadeau OW, Carlson GM (2008) Structural evidence for co-evolution of the regulation of contraction and energy production in skeletal muscle. J Mol Biol 377:623–629.
10. Nadeau OW, Carlson GM, Gogol EP (2002) A Ca^{2+}-dependent global conformational change in the 3D structure of phosphorylase kinase obtained from electron microscopy. Structure 10:23–32.
11. Rice NA, Nadeau OW, Yang Q, Carlson GM (2002) The calmodulin-binding domain of the catalytic gamma subunit of phosphorylase kinase interacts with its inhibitory α subunit: evidence for a Ca^{2+} sensitive network of quaternary interactions. J Biol Chem 277:14681–14687.
12. Nadeau OW, Anderson DW, Yang Q, Artigues A, Paschall JE, Wyckoff GJ, McClintock JL, Carlson GM (2007) Evidence for the location of the allosteric activation switch in the multisubunit phosphorylase kinase complex from mass spectrometric identification of chemically crosslinked peptides. J Mol Biol 365:1429–1445.
13. Wilkinson DA, Norcum MT, Fizgerald TJ, Marion TN, Tillman DM, Carlson GM (1997) Proximal regions of the catalytic γ and regulatory β subunits on the interior lobe face of phosphorylase kinase are structurally coupled to each other and with enzyme activation. J Mol Biol 265:319–329.
14. Thompson JA, Nadeau OW, Carlson GM (2015) A model for activation of the hexadecameric phosphorylase kinase complex deduced from zero-length oxidative crosslinking. Protein Sci 24:1956–1963.
15. Ayers NA, Nadeau OW, Read MW, Ray P, Carlson GM (1998) Effector-sensitive cross-linking of phosphorylase b kinase by the novel cross-linker 4-phenyl-1,2,4-triazoline-3,5-dione. Biochem J 331:137–141.
16. Nadeau OW, Sacks DB, Carlson GM (1997) The structural effects of endogenous and exogenous Ca2+/calmodulin on phosphorylase kinase. J Biol Chem 272: 26202–26209.
17. Nadeau OW, Sacks DB, Carlson GM (1997) Differential affinity cross-linking of phosphorylase kinase conformers by the geometric isomers of phenylenedimaleimide. J Biol Chem 272:26196–26201.
18. Nadeau OW, Traxler KW, Carlson GM (1998) Zero-length crosslinking of the beta subunit of phosphorylase kinase to the N-terminal half of its regulatory α subunit. Biochem Biophys Res Commun 251:637–641.
19. Nadeau OW, Traxler KW, Fee LR, Baldwin BA, Carlson GM (1999) Activators of phosphorylase kinase alter the cross-linking of its catalytic subunit to the C-terminal one-sixth of its regulatory α subunit. Biochemistry 38:2551–2559.
20. Lane LA, Nadeau OW, Carlson GM, Robinson CV (2012) Mass spectrometry reveals differences in stability and subunit interactions between activated and nonactivated conformers of the (alphabetagammadelta)4 phosphorylase kinase complex. Mol Cell Proteomics 11:1768–1776.
21. Nadeau OW, Lane LA, Xu D, Sage J, Priddy TS, Artigues A, Villar MT, Yang Q, Robinson CV, Zhang Y, Carlson GM (2012) Structure and location of the regulatory β subunits in the $(\alpha\beta\gamma\delta)_4$ phosphorylase kinase complex. J Biol Chem 287:36651–36661.
22. Norcum MT, Wilkinson DA, Carlson MC, Hainfeld JF, Carlson GM (1994) Structure of phosphorylase kinase. A three-dimensional model derived from stained and unstained electron micrographs. J Mol Biol 241:94–102.
23. Wilkinson DA, Marion TN, Tillman DM, Norcum MT, Hainfeld JF, Seyer JM, Carlson GM (1994) An epitope proximal to the carboxyl terminus of the α-subunit is located near the lobe tips of the phosphorylase kinase hexadecamer. J Mol Biol 235:974–982.
24. Traxler KW, Norcum MT, Hainfeld JF, Carlson GM (2001) Direct visualization of the calmodulin subunit of phosphorylase kinase via electron microscopy following subunit exchange. J Struct Biol 135:231–238.
25. Chattopadhyaya R, Meador WE, Means AR, Quiocho FA (1992) Calmodulin structure refined at 1.7 A resolution. J Mol Biol 228:1177–1192.
26. Owen DJ, Noble ME, Garman EF, Papageorgiou AC, Johnson LN (1995) Two structures of the catalytic domain of phosphorylase kinase: an active protein kinase complexed with substrate analogue and product. Structure 3:467–482.
27. Rimmer MA, Nadeau OW, Yang J, Artigues A, Zhang Y, Carlson GM (2017) (in press) The structure of the large regulatory α subunit of phosphorylase kinase examined by modeling and hydrogen-deuterium exchange. Protein Sci.
28. Pascal BD, Chalmers MJ, Busby SA, Griffin PR (2009) HD desktop: an integrated platform for the analysis and visualization of H/D exchange data. J Am Soc Mass Spectrom 20:601–610.
29. Kan ZY, Walters BT, Mayne L, Englander SW (2013) Protein hydrogen exchange at residue resolution by proteolytic fragmentation mass spectrometry analysis. Proc Natl Acad Sci USA 110:16438–16443.
30. Roy A, Kucukural A, Zhang Y (2010) I-TASSER: a unified platform for automated protein structure and function prediction. Nat Protoc 5:725–738.
31. Yang J, Yan R, Roy A, Xu D, Poisson J, Zhang Y (2015) The I-TASSER Suite: protein structure and function prediction. Nat Meth 12:7–8.

32. Zhang Y (2008) I-TASSER server for protein 3D structure prediction. BMC Bioinformat 9:40.
33. Carriere C, Jonic S, Mornon JP, Callebaut I (2008) 3D mapping of glycogenosis-causing mutations in the large regulatory α subunit of phosphorylase kinase. Biochim Biophys Acta 1782:664–670.
34. Pallen MJ (2003) Glucoamylase-like domains in the α- and β-subunits of phosphorylase kinase. Protein Sci 12:1804–1807.
35. Mizuno M, Tonozuka T, Suzuki S, Uotsu-Tomita R, Kamitori S, Nishikawa A, Sakano Y (2004) Structural insights into substrate specificity and function of glucodextranase. J Biol Chem 279:10575–10583.
36. Nadeau OW, Liu W, Boulatnikov IG, Sage JM, Peters JL, Carlson GM (2010) The glucoamylase inhibitor acarbose is a direct activator of phosphorylase kinase. Biochemistry 49:6505–6507.
37. Liu HL, Wang WC (2003) Predicted unfolding order of the 13 α-helices in the catalytic domain of glucoamylase from Aspergillus awamori var. X100 by molecular dynamics simulations. Biotechnol Prog 19:1583–1590.
38. Fitzgerald TJ, Carlson GM (1984) Activated states of phosphorylase kinase as detected by the chemical cross-linker 1,5-difluoro-2,4-dinitrobenzene. J Biol Chem 259:3266–3274.
39. Trempe MR, Carlson GM (1987) Phosphorylase kinase conformers. Detection by proteases. J Biol Chem 262: 4333–4340.
40. Rimmer MA, Artigues A, Nadeau OW, Villar MT, Vasquez-Montes V, Carlson GM (2015) Mass spectrometric analysis of surface-exposed regions in the hexadecameric phosphorylase kinase complex. Biochemistry 54:6887–6895.
41. Hook SS, Means AR (2001) Ca^{2+}/CaM-dependent kinases: from activation to function. Annu Rev Pharmacol Toxicol 41:471–505.
42. Manning G, Whyte DB, Martinez R, Hunter T, Sudarsanam S (2002) The protein kinase complement of the human genome. Science 298:1912–1934.
43. de Diego I, Kuper J, Bakalova N, Kursula P, Wilmanns M (2010) Molecular basis of the death-associated protein kinase-calcium/calmodulin regulator complex. Sci Signal 3:ra6.
44. Rellos P, Pike AC, Niesen FH, Salah E, Lee WH, von Delft F, Knapp S (2010) Structure of the CaMKIIdelta/calmodulin complex reveals the molecular mechanism of CaMKII kinase activation. PLoS Biol 8:e1000426.
45. Lowe ED, Noble ME, Skamnaki VT, Oikonomakos NG, Owen DJ, Johnson LN (1997) The crystal structure of a phosphorylase kinase peptide substrate complex: kinase substrate recognition. embo J 16:6646–6658.
46. Kornev AP, Taylor SS (2015) Dynamics-driven allostery in protein kinases. Trends Biochem Sci 40:628–647.
47. Kornev AP, Haste NM, Taylor SS, Eyck LF (2006) Surface comparison of active and inactive protein kinases identifies a conserved activation mechanism. Proc Natl Acad Sci USA 103:17783–17788.
48. Kornev AP, Taylor SS, Ten Eyck LF (2008) A helix scaffold for the assembly of active protein kinases. Proc Natl Acad Sci USA 105:14377–14382.
49. Taylor SS, Kornev AP (2011) Protein kinases: evolution of dynamic regulatory proteins. Trends Biochem Sci 36: 65–77.
50. Meharena HS, Chang P, Keshwani MM, Oruganty K, Nene AK, Kannan N, Taylor SS, Kornev AP (2013) Deciphering the structural basis of eukaryotic protein kinase regulation. PLoS Biol 11:e1001680.
51. Azam M, Seeliger MA, Gray NS, Kuriyan J, Daley GQ (2008) Activation of tyrosine kinases by mutation of the gatekeeper threonine. Nat Struct Mol Biol 15: 1109–1118.
52. Yang J, Wu J, Steichen JM, Kornev AP, Deal MS, Li S, Sankaran B, Woods VL, Jr, Taylor SS (2012) A conserved Glu-Arg salt bridge connects coevolved motifs that define the eukaryotic protein kinase fold. J Mol Biol 415:666–679.
53. Resing KA, Ahn NG (1998) Deuterium exchange mass spectrometry as a probe of protein kinase activation. Analysis of wild-type and constitutively active mutants of MAP kinase kinase-1. Biochemistry 37:463–475.
54. Sours KM, Kwok SC, Rachidi T, Lee T, Ring A, Hoofnagle AN, Resing KA, Ahn NG (2008) Hydrogen-exchange mass spectrometry reveals activation-induced changes in the conformational mobility of p38alpha MAP kinase. J Mol Biol 379:1075–1093.
55. Taylor SS, Yang J, Wu J, Haste NM, Radzio-Andzelm E, Anand G (2004) PKA: a portrait of protein kinase dynamics. Biochim Biophys Acta 1697:259–269.
56. Kannan N, Neuwald AF (2005) Did protein kinase regulatory mechanisms evolve through elaboration of a simple structural component?. J Mol Biol 351:956–972.
57. Cox S, Johnson LN (1992) Expression of the phosphorylase kinase gamma subunit catalytic domain in Escherichia coli. Protein Eng 5:811–819.
58. Priddy TS, Price ES, Johnson CK, Carlson GM (2007) Single molecule analyses of the conformational substates of calmodulin bound to the phosphorylase kinase complex. Protein Sci 16:1017–1023.
59. Schumacher MA, Rivard AF, Bachinger HP, Adelman JP (2001) Structure of the gating domain of a Ca2+-activated K+ channel complexed with Ca^{2+}/calmodulin. Nature 410:1120–1124.
60. Vlach J, Samal AB, Saad JS (2014) Solution structure of calmodulin bound to the binding domain of the HIV-1 matrix protein. J Biol Chem 289:8697–8705.
61. Ledoux J, Bonev AD, Nelson MT (2008) Ca2+-activated K+ channels in murine endothelial cells: block by intracellular calcium and magnesium. J Gen Physiol 131:125–135.
62. Ramachandran C, Goris J, Waelkens E, Merlevede W, Walsh DA (1987) The interrelationship between cAMP-dependent alpha and beta subunit phosphorylation in the regulation of phosphorylase kinase activity. Studies using subunit specific phosphatases. J Biol Chem 262: 3210–3218.
63. Brostrom CO, Hunkeler FL, Krebs EG (1971) The relation of skeletal muscle phosphorylase kinase by Ca^{2+}. J Biol Chem 246:1961–1967.